Thompson, J, Power, R, Mercieca-Spiteri, B, Magnussen, J, Pardey, M, Buck, LT, Stock, J, McLaughlin, R, Stoddart, S and Malone, C

Analysis of periosteal lesions from commingled human remains at the Xagħra Circle hypogeum reveals the first case of probable scurvy from Neolithic Malta

Received: 9 May 2021 | Revised: 19 July 2021 | Accepted: 25 August 2021

DOI: 10.1002/oa.3040

RESEARCH ARTICLE

Analysis of periosteal lesions from commingled human remains at the Xagħra Circle hypogeum reveals the first case of probable scurvy from Neolithic Malta

Jess E. Thompson[1] | Ronika K. Power[1,2] | Bernardette Mercieca-Spiteri[3] | John S. Magnussen[4] | Margery Pardey[4] | Laura T. Buck[1,5] | Jay T. Stock[6,7] | T. Rowan McLaughlin[8,9] | Simon Stoddart[1] | Caroline Malone[8]

[1]McDonald Institute for Archaeological Research, University of Cambridge, Cambridge, UK

[2]Department of History and Archaeology, Macquarie University, Sydney, New South Wales, Australia

[3]Superintendence of Cultural Heritage, Valletta, Malta

[4]Department of Clinical Medicine, Faculty of Medicine, Health and Human Sciences, Macquarie University, Sydney, New South Wales, Australia

[5]School of Biological and Environmental Sciences, Liverpool John Moores University, Liverpool, UK

[6]Department of Anthropology, Western University, London, Ontario, Canada

[7]Department of Archaeology, Max Planck Institute for the Science of Human History, Jena, Germany

[8]School of Natural and Built Environment, Queen's University Belfast, Belfast, UK

[9]The British Museum, London, UK

Correspondence
J. E. Thompson, McDonald Institute for Archaeological Research, University of Cambridge, Cambridge, UK.
Email: jet71@cam.ac.uk

Funding information
FP7 Ideas: European Research Council, Grant/Award Number: 323727; Magdalene College, University of Cambridge; Arts and Humanities Research Council

Abstract

Objectives: Palaeopathological analysis is key for characterising population health at the individual level and across large assemblages but is rarely exploited to unite the remains of disarticulated individuals. This study explores the potential for individual identification through differential diagnosis of periosteal lesions in a commingled deposit, both to ascertain the number of individuals represented and provide a differential diagnosis.

Materials and Methods: The late Neolithic Xagħra Circle hypogeum on Gozo contains the remains of more than 800 individuals, most of which were transformed to a collective disarticulated assemblage. Across the excavated population, pathological observations are strikingly low. In one specific 1 × 1-m area in a single stratigraphic context, fragmented and disarticulated cranial and post-cranial non-adult bones were identified that displayed periosteal new bone formation. To aid differential diagnosis, macroscopic analysis, taphonomic analysis and micro-computed tomography (μCT) imaging were integrated.

Results: This approach, when combined with osteobiographical analyses, reveals that the elements most likely derive from one individual, a young child, who presents a probable case of scurvy. The potential for micronutrient co-morbidities are explored, but without further microscopic study it cannot be determined if this individual also experienced iron-deficiency anaemia and/or rickets.

Discussion: In the context of the Mediterranean and Europe in later prehistory, reported cases of scurvy are currently low and often reveal periods of environmental instability and resource insufficiency. Our finding of non-adult scurvy in late 3rd millennium BC Malta contributes to a developing picture of an increasingly unstable palaeoenvironment and declining population health at this time, although it may also indicate an individual case of poor childhood health within this broader context.

KEYWORDS
commingled remains, Mediterranean, Micro-CT, Neolithic, palaeopathology, periosteal lesions, scurvy, vitamin C deficiency

1 | INTRODUCTION

Despite their ubiquitous presence in skeletal collections, differential diagnosis of periosteal lesions is especially challenging because of their wide range of potential aetiologies (Ortner, 2003, p. 206; Weston, 2012). In deposits of commingled remains, differential diagnosis is limited by our inability to recognise discrete individuals across which pathogenic processes can be traced. Typically, only uncommon or more severe pathological lesions are likely to yield a diagnosis and lead to individual identification (e.g. Cunha, 2006). Within large assemblages of human remains, palaeopathological analysis is commonly used to characterise population health; only rarely have pathological lesions provided the opportunity to unite the remains of disarticulated individuals (González-Reimers et al., 2015; Ortner, 2003). Here, we assess periosteal lesions from a range of disarticulated and fragmented bones found within one specific 1 × 1-m area in one archaeological context at the collective deposition site of the Xagħra Circle (Gozo). The high number of non-adult elements displaying periosteal lesions within this area allows us to explore the potential of macroscopic and microscopic analysis of pathological lesions to produce differential diagnoses which constrain the number of identifiable individuals.

The human remains from the Xagħra Circle hypogeum, dating to the late Neolithic "Temple Period" of Maltese prehistory (3800–2200 cal BC), have recently undergone detailed re-analysis, including aDNA, dental anthropology and modification, isotopes ($\delta^{15}N$, $\delta^{13}C$, $\delta^{18}O/^{16}O$, $\delta^{87}Sr/^{86}Sr$), funerary taphonomy, long bone cross-sectional geometry, and palaeopathology (Stoddart et al., in press). The complete assemblage of more than 200,000 bone fragments was visually examined (by RKP and BMS) to identify all examples of severe palaeopathological lesions and trauma (Mercieca-Spiteri et al., in press). Within the full assemblage, periosteal lesions were markedly low, but a notable concentration occurred in one archaeological context (960), dated towards the end of the site's use (Power et al., in press a). From this context, six skeletal elements presenting periosteal lesions were selected for detailed analysis due to their deposition within a discrete 1 × 1-m area. We employed macroscopic observation, taphonomic analysis and μCT imaging to aid differential diagnosis. This approach demonstrates the significant role of palaeopathological analysis in the study of commingled assemblages.

1.1 | Archaeological context of the Xagħra Circle hypogeum

The late Neolithic period on the Maltese islands (3800–2200 cal BC) is commonly known as the "Temple Period" because of the construction of large monumental buildings which hosted communal gatherings and feasts (Barratt et al., 2020). Throughout this time, collective deposition was practised in rock-cut tombs, caves and hypogea, with the scale of deposition increasing from 2900 cal BC (Malone et al., 2019). The Xagħra Circle hypogeum (Figure 1a) comprises a series of interconnecting caves and niches used for complex multi-stage funerary rituals (Malone et al., 2009). Radiocarbon dating has revealed that deposition of the dead peaked between 2600–2500 cal BC and tapered off by 2300 cal BC (Malone et al., 2019). All human bone was excavated in 1 × 1-m grid squares and planned to scale at each level (usually 10 cm depth), providing high resolution spatial data on the in situ position of many of the skeletal remains (Malone et al., 2009). Based on the representation of crania, the excavated remains produced an estimate of 822 deposited individuals (Stoddart, Barber, et al., 2009, p. 319). Given that the hypogeum is not fully excavated, and the process of successive deposition has suppressed the identifiable minimum number of individuals (Robb, 2016), the original number of individuals deposited could have been substantially larger. To our knowledge, the Xagħra Circle is one of the largest and longest used Neolithic burial sites in Europe and is of international importance.

Visitors to the hypogeum descended first into the central area of the West Cave referred to as the "Shrine." The Shrine area contained some primary interments, and was furnished with megalithic shelving (possibly displaying crania) and screens (Malone et al., 2019; Stoddart, Malone, et al., 2009; Thompson et al., 2020). Later deposits in the Shrine in contexts (960) and (1206) are characterised by predominantly disarticulated remains (Stoddart, Malone, et al., 2009, pp. 145–9) and small bones are under-represented, indicating a variety of depositional modes, including disturbed primary interments, the clustering of crania, and selective removal of bone (Thompson, 2020).

The original analysis of the excavated assemblage noted a low prevalence of pathological lesions (Stoddart et al., 2009a), suggesting that the majority of the interred population were more likely to have died from acute conditions (Power et al., in press a). The highest incidences of pathological lesions were observed in contexts (783) and (960), formed during the Late use phase of the site (Stoddart et al., 2009a). Recent analyses reveal increased evidence for enamel hypoplasia between 2550 and 2500 cal BC (Power et al., in press b), contemporary with these contexts and concomitant with dietary and subsistence practice changes (McLaughlin et al., 2020). Increased attention has recently been paid to evidence for osteoporosis in the Circle population, including vertebral crush fractures (Power et al., in press b). These indicators of general nutritional and environmental stress, coalescing several centuries prior to the end of the site's use, provide the social and physiological context under which the elements considered below are interpreted.

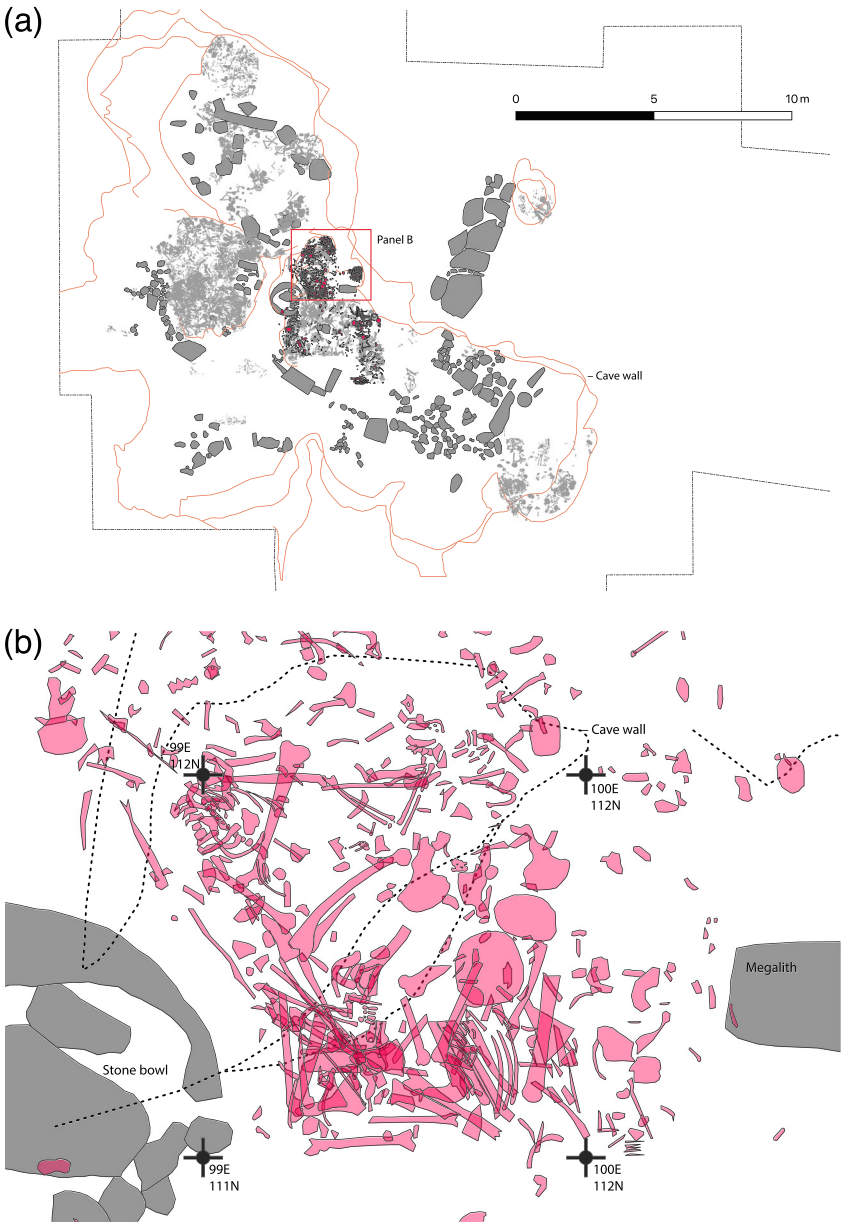

FIGURE 1 Plan of the excavated limits of the Xagħra Circle hypogeum, displaying (a) location of megaliths and human remains excavated in the latter years; (b) area under study in context (960) from the central "Shrine" Zone. Map by Rowan McLaughlin [Colour figure can be viewed at wileyonlinelibrary.com]

2 | MATERIALS AND METHODS

2.1 | Remains presenting periosteal lesions

Within the Shrine area, context (960) contained almost 12,000 fragments of human bone, and only one articulated skeleton remained undisturbed following their deposition (Stoddart et al. 2009b, 149). This context is dated between 2500–2400 cal BC, although some remains were residual and dated as early as 2850 cal BC (Malone et al., 2019). We infer that part of the deposit represents the clearance of remains initially placed much earlier in other areas of the hypogeum. From this context, numerous adult and non-adult bone fragments exhibiting extensive periosteal new bone formation were identified post-excavation. This study concentrates on the non-adult remains excavated from one specific 1×1 m-area (Figure 1b).

Periosteal lesions were observed on 10 fragments representing 6 elements (Table 1). In the adjacent 1×1-m area, further bone fragments exhibiting periosteal lesions, deriving from multiple adult individuals, were found (for differential diagnosis, see Power et al., in press a). Most of the non-adult remains are cranial and represent the facial skeleton. It is not possible to directly re-fit the right orbit or left zygoma to the largest portions of the frontal bone, but based on both morphology and depositional location, it is highly probable they derive from one individual. Portions of a right and left rib and ulna are also present. All elements (except the right rib, for which this information is lacking) were assigned the same unit number upon excavation, indicating their close spatial association.

TABLE 1 Summary of non-adult pathological elements from context (960)

Element and ID	Side	Preservation	Description	Age
Frontal (FB0039; FB0040)	Axial	Fair	Several fragments of frontal which refit. Some taphonomic damage to lesions and element	Young child
Zygoma (FB0041)	Left	Fair	Complete except for fragmented frontal process	Young child
Mandible (FB0042)	Axial	Good	Two fragments which refit	Young child
Rib (FB0043)	Left	Good	Middle-lower order rib diaphysis	Young child
Rib (FB0044)	Right	Fair	Lower order rib diaphysis	Young child
Ulna (FB0045)	Unknown	Fair	Fragment of distal third of diaphysis	Young child

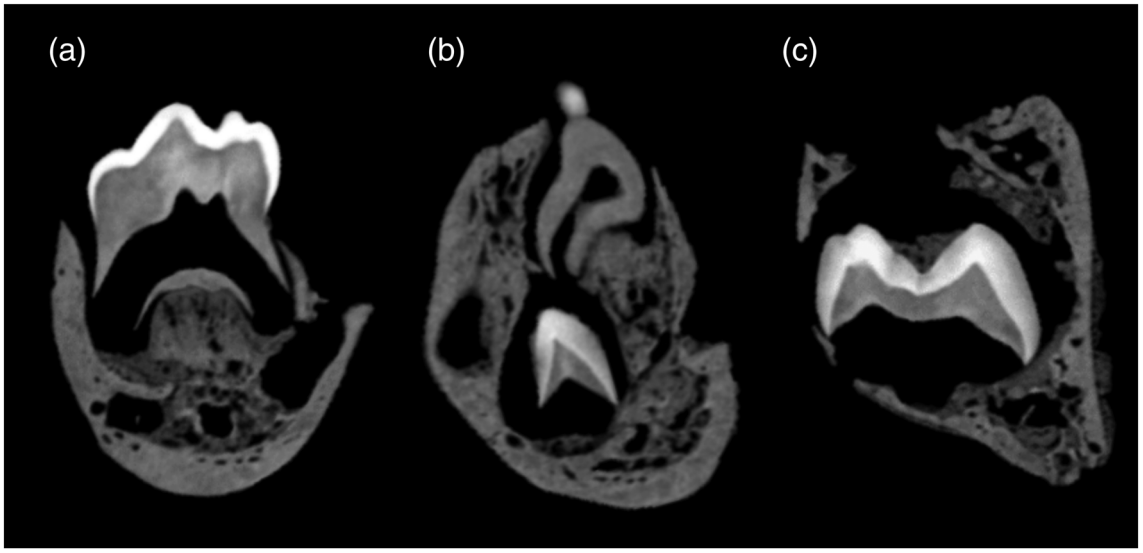

FIGURE 2 μCT cross-sections of the mandible (FB0042), showing (a) eruption of the deciduous left second molar; (b) eruption of the deciduous right first molar and development of the permanent right first premolar; (c) development of the permanent right first molar. Cross-sectional images produced by John S. Magnussen

Mandibular dental eruption indicates an age at death of 2 years (±8 months) (Ubelaker, 1989). This individual corresponds to the age range for which AlQahtani et al. (2010) admit a smaller available sample size from the reference material used to develop their dental eruption chart (6 months to 2 years). The dental development of this individual is more advanced than that represented by the midpoint age 1.5 years, yet the apices of the deciduous anterior dentition cannot be assessed with reference to the next midpoint age 2.5 years because of post-mortem loss. Assessed via μCT, the roots of the deciduous left second molar are ¼ developed (Figure 2a), the deciduous right first molar is erupted with the roots ¾ developed, the crown of the permanent right first premolar has completed development (Figure 2b), and the crown of the permanent right first molar is complete (Figure 2c). Almost complete closure of the metopic suture alongside closure of the anterior fontanelle and mandibular symphysis suggests a minimum age of 2–4 years, and the proportions of the zygoma are characteristic of individuals of 2–3 years of age (Scheuer & Black, 2000, pp. 108, 124). The extant rib shafts demonstrate torsion and suggest the individual was between 1 and 3 years of age at death (Scheuer & Black, 2000, p. 241).

2.2 | Macroscopic and micro-CT analysis

The lesions were observed macroscopically and using a hand lens (×10 magnification). Details of the affected element, side, location, and type of lesion were recorded (Buikstra & Ubelaker, 1994; Weston, 2012). The lesions were defined as active when observed to be raised, discoloured, and extensively vascularised (Mann & Hunt, 2012, p. 157). Healed lesions were observed to be more continuous in colour and texture with the surrounding unaffected cortex. The maximum extent of the lesions was measured to the nearest 0.1 mm using digital callipers on flat planes and to the nearest millimetre using a hand tape on irregular surfaces. Post-mortem fragmentation and taphonomic erosion truncated the lesions on all fragments, obfuscating full observation. Brief summaries of the lesions are included below (see Power et al., in press a, for full macroscopic and radiological descriptions). Given the disarticulated nature of these elements, the often non-specific aetiology of periosteal lesions, and the challenges of distinguishing between normal and pathological periosteal bone deposition in infants and young children (Rittemard et al., 2019), all elements were scanned via micro-

computed tomography (μCT), to enable visualisation of the internal bone microstructure.

These elements were transported from the National Museum of Archaeology, Valletta, Malta (by BMS) with the permission of Heritage Malta and the Superintendence of Cultural Heritage, Malta, to carry out μCT scanning at the Cambridge Biotomography Centre, University of Cambridge, UK. Scans were taken with a Nikon Metrology XT H 225 ST (by LTB) and have voxel sizes ranging from 0.06 to 0.12 μm^3 (to two decimal places). The resulting scans were processed using 3D Slicer (Fedorov et al., 2012), RadiAnt (Medixant, Promienista, Poland) and AW Server (GE Medical Systems, Milwaukee, USA) at the Macquarie Medical Imaging Unit, Macquarie University Hospital (by MP and JSM). Analysis and differential diagnoses were carried out collaboratively (JSM, RKP and JET).

3 | MACROSCOPIC AND RADIOLOGICAL OBSERVATIONS OF PATHOLOGY

Ten fragments representing a minimum of six skeletal elements of at least one young child presented multifocal periosteal lesions (Table 2). There were no observations of fracture, cloaca or sequestra on any fragments, although it cannot be ruled out that such features were present on the elements or fragments which have not been preserved. The similar developmental stage of the non-adult remains, as well as the remarkably consistent presentation of the lesions macroscopically and radiologically, suggests they could derive from a single individual, but this cannot be verified without biomolecular analyses. In the following descriptions, macroporosity is defined as pores >1 mm in diameter, while micropores are <1 mm in diameter.

3.1 | Frontal bone (FB0039, FB0040) and zygoma (FB0041)

The inner and outer tables of the frontal squama are well-preserved although the condition of the cortex on the left supra-orbital margin deteriorated towards the midline (Figure 3a), and the outer table is irregular and thin in the region of the right supra-orbital margin (Figure 3b). Superior to the frontonasal suture, the outer table of the frontal bone presents a diffuse, poorly demarcated lesion characterised by small radiolucent holes when viewed via μCT, although only sparse macroporosity is observed macroscopically (Figure 3c), and the trabeculae are in good condition. The appearance of radiolucent holes is referred to as "moth-eaten" in radiological descriptions, describing a true permeative process of bone (Brant & Helms, 2012). Extensive deposits of plaque-like finely woven bone, spicules and microporosity are present on the lateral aspects of the right and left supraorbital margins (Figure 3d,e) and across the surface of the right and left orbital roofs (Figure 3f,g). Micro-CT revealed the greatest degree of spiculation close to, and involving, the frontal sinus. In cross-section, alongside pronounced spiculation, the cortices surrounding the frontal sinus presented similar lesions as described for the outer table: diffuse poorly-demarcated small radiolucent holes, and the trabeculae were eroded (Figure 3h). Extensive lesions across the zygoma comprised dense spiculated bone, occasionally perpendicular to the cortex on the anterior aspect, while the posterior (internal) surface presented diffuse microporosity (Figure 4a,b). Considerable cortical demineralisation is evident via μCT, but the trabeculae are relatively well-preserved, and the margins of nutrient foramina and vascular channels remain intact.

3.2 | Mandible (FB0042)

On the mandible, focal areas of reactive bone were present alongside micro- and macro-porosity and associated with cortical bone degradation. Small spiculations are preserved on the anterior aspect of the mandibular corpus, superficial to the alveoli containing the developing permanent canines. Both right and left mandibular angles display periosteal new bone on the buccal and lingual aspects (Figure 4c–g). The lesions are more widespread on the left side, particularly on the buccal aspect. When viewed via μCT, extensive bone loss on the buccal

TABLE 2 Summary of lesion/s location, type and healing status on all non-adult elements

Element	Side	Bilateral?	Lesion/s location	Lesion type	Healing status
Frontal	Axial	Yes	Floor of anterior cranial fossa; frontal sinus[a]; orbital roofs; surrounding supra-orbital margins, endocranial aspect of frontal squama	Proliferative	Active
Zygoma	Left	Unknown	Full extent of anterior, posterior and superior aspects	Mixed	Mixed
Mandible	Axial	Yes	Anterior and lateral aspects of the corpus; right coronoid process; buccal and lingual aspects of the rami, including gonial angle and mylohyoid groove	Mixed	Mixed
Rib (middle-lower order)	Left	Unknown	Pleural and external aspects of corpus	Mixed	Mixed
Rib (lower order)	Right	Unknown	Pleural, external and superior aspects of corpus	Mixed	Mixed
Ulna	Unknown	Unknown	Encircling extant portion of the distal half of the diaphysis. Localised elevations from the cortex indicate subperiosteal haematoma[a]	Proliferative	Active

[a]Lesion only visible via micro-CT.

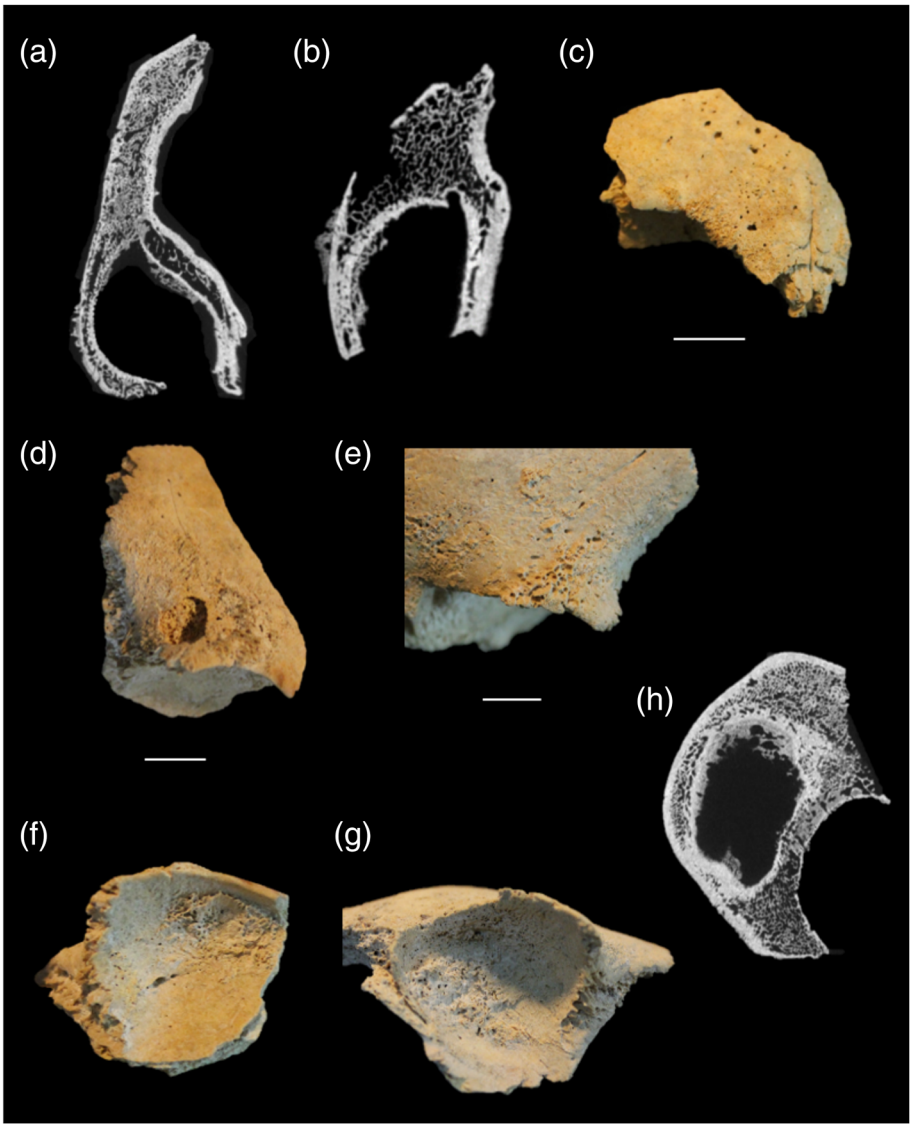

FIGURE 3 Images of non-adult cranial elements displaying periosteal lesions diagnostic and suggestive of scurvy, (a) μCT sagittal cross-section of through the glabella and left orbit (FB0039); (b) μCT sagittal cross-section through lateral aspect of right orbit (FB0040); (c) fragment of frontal bone displaying glabella region, frontonasal suture and extant medial portion of right supraorbital margin (FB0039); (d) lateral aspect of right supraorbital margin (FB0039); (e) lateral aspect of left supraorbital margin (FB0040); (f) inferior view of left orbital roof (FB0039); (g) inferior view of right orbital roof (FB0040); (h) μCT orthogonal plane cross-section of left frontal sinus (FB0039). Scale bar: 1 cm (photographs only). Photographs by Jess E. Thompson and cross-sectional images produced by John S. Magnussen [Colour figure can be viewed at wileyonlinelibrary.com]

surface of the right ramus was observed and, on the left ramus, the cortices of the inner and outer table are demineralised and thinned. Both healing and active lesions are present, with periosteal new bone located close to the alveoli on the buccal aspect of the posterior dentition and expressed bilaterally. Most deciduous dentition appears to have been lost post-mortem (lower left incisors, canine and first molar, lower right incisors, canine and second molar), as there is no evidence of alveolar resorption.

3.3 | Left rib (FB0043) and right rib (FB0044)

Both ribs display healing or healed lesions on the external aspect, with active woven bone on the pleural surfaces. The right rib presents widespread but subtle circumferential spiculated deposits of new bone (Figure 5a). The left rib presents patchy new bone deposition almost circumferentially with involvement of the pleural (Figure 5b) and external surfaces on the medial and lateral ends of the extant portion of the element. Lesions on the pleural surface are spiculated towards the lateral aspect of the extant fragment, with separation in parts between the cortex and the new bone identified via μCT.

3.4 | Ulna (FB0045)

Thick deposits of woven bone envelope the full extent of the ulna fragment (maximum length 55.5 mm), which is encircled with radiating spiculations presenting a "frosted" appearance when observed macroscopically (Figure 5c). On the distal third of the diaphysis, μCT imaging showed that segments of the periosteal new bone are elevated from the underlying cortex (Figure 5d–f). As a result of taphonomic erosion of the distal metaphysis, the element cannot be assessed for diagnostic radiological features, including Pelkan spurs, Wimberger's ring, metaphyseal white lines ("white line of Frankel") and the Trümmerfeld zone. No healthy cortex remains and there has been significant

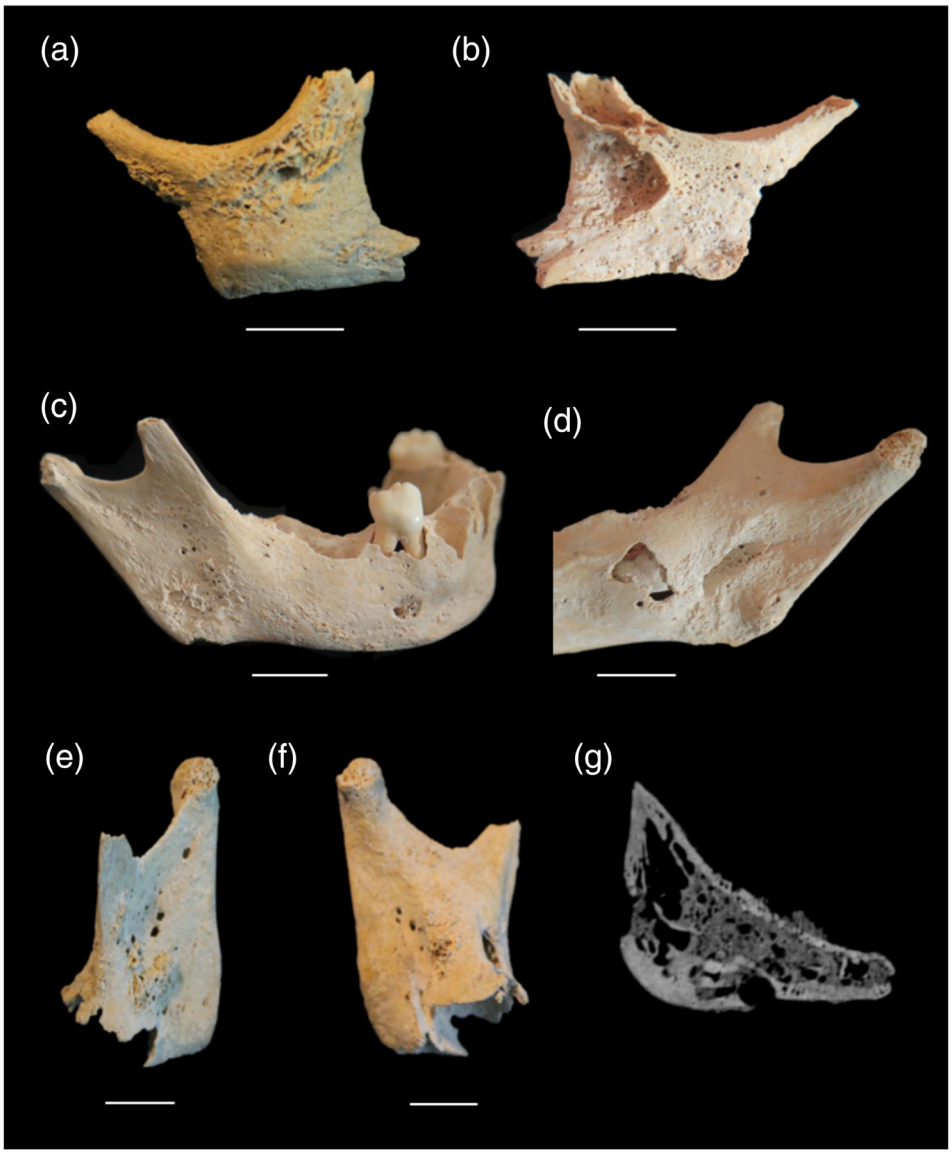

FIGURE 4 Images of non-adult elements displaying periosteal lesions diagnostic and suggestive of scurvy, (a) anterior view of left zygoma (FB0042); (b) posterior view of left zygoma; (c) right lateral view of mandible (FB0042); (d) right medial view of mandible; (e) antero-lateral view of left mandibular ramus; (f) medial view of left mandibular ramus; (g) μCT sagittal cross-section through right ramus. Scale bar: 1 cm (photographs only). Photographs by Jess E. Thompson and cross-sectional images produced by John S. Magnussen [Colour figure can be viewed at wileyonlinelibrary.com]

cortical bone loss. Post-depositional taphonomic processes have eroded most of the trabeculae, although some are preserved towards the distal portion of the extant diaphysis; as such, the degree of trabecular involvement cannot be characterised.

4 | DIFFERENTIAL DIAGNOSIS

Periosteal new bone forms as a result of numerous processes which stimulate and inflame the periosteum, with diverse aetiologies such as circulatory and haematological disorders, joint, infectious, metabolic and neoplastic diseases, skeletal dysplasias, and trauma (Aufderheide & Rodríguez-Martín, 1998; Mann & Hunt, 2012; Ortner, 2003; Rana et al., 2009; Weston, 2008, 2012). The location, severity, expression and distribution of periosteal lesions may indicate their pathogenesis (Pinheiro et al., 2004), although Weston (2008, 2009) reports that the morphology of periosteal lesions relates more closely to healing status and chronicity than aetiology. In infants and children, however, new bone formation is an ongoing process as part of normal appositional growth, usually resulting in the deposition of smooth, single layers of bone (Lewis, 2018; Weston, 2012). As the periosteum is loosely attached to the cortex, it is more susceptible to lifting and can remodel more rapidly and aggressively than in adults (Jones, 1998; Rittemard et al., 2019; Shopfner, 1966).

Clinically, periosteal lesions are classified as benign or aggressive based on their appearance (Rana et al., 2009; Richardson, 2001). Similar lesions may be observed across both benign and aggressive cases, but benign processes are generally associated with solid and thick periosteal new bone. Aggressive and rapid new bone formation often presents as spiculated hair-on-end or sunburst deposits of bone perpendicular or angulated to the original cortex. Proliferative lesions may be attributed to inflammatory processes or subperiosteal haematoma (Ortner, 2003, p. 88). Unilateral distribution of lesions often indicates localised processes, such as infection, trauma or tumour, whereas bilateral lesions are more likely to be systemic (Ortner, 2003, pp. 206–7; Rana et al., 2009; Weston, 2012, p. 504).

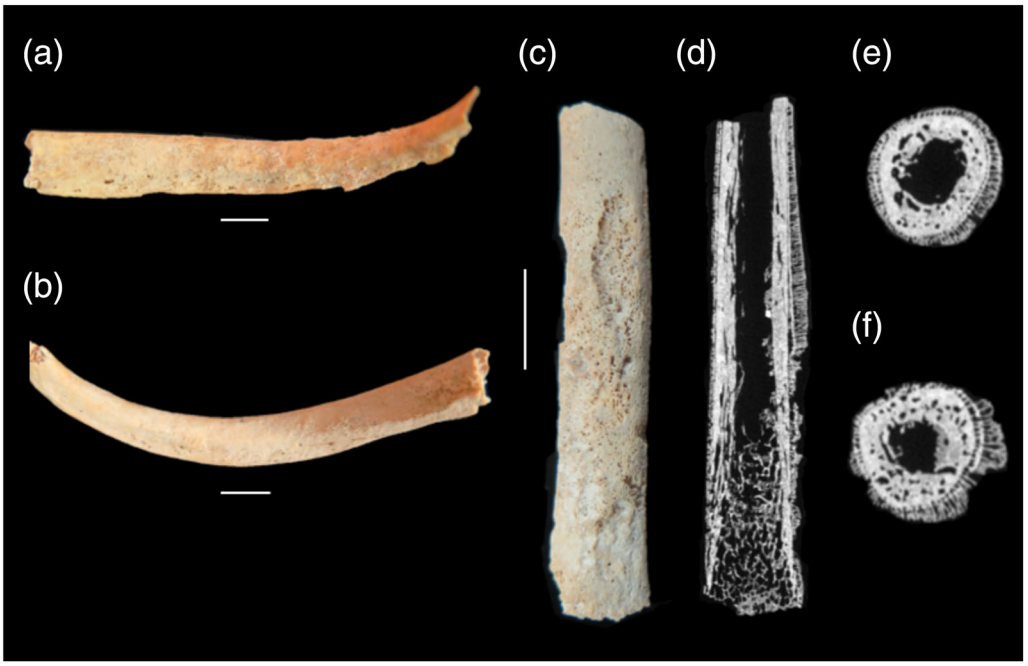

FIGURE 5 Images of non-adult post-cranial elements displaying periosteal lesions diagnostic and suggestive of scurvy, (a) internal aspect of right rib (FB0044); (b) internal aspect of left rib (FB0043); (c) distal ulna fragment (FB0045); (d) μCT sagittal cross-section of ulna; (e) transverse cross-section of ulna at proximal aspect of extant element; (f) transverse cross-section of ulna at mid-point of extant portion of element. Scale bar: 1 cm (photographs only). Photographs by Jess E. Thompson and cross-sectional images produced by John S. Magnussen [Colour figure can be viewed at wileyonlinelibrary.com]

Of key importance for differential diagnoses are knowledge of the individual's age, sex, and health status (Weston, 2008). Given the age estimate of 2–4 years for all non-adult elements, and the similar presentation of the periosteal lesions, they are considered as representing one young child. The distribution of the lesions, including bilateral involvement of the orbital roofs, supra-orbital margins, and mandibular rami, intrusion into the frontal sinus, as well as the spiculated character of the reactive bone, indicates an infectious, neoplastic or metabolic pathogenesis (Brickley & Ives, 2008; Ortner, 2003; Rana et al., 2009). Intra- or peri-cranial infection, metastatic neuroblastoma, meningitis, infantile cortical hyperostosis (ICH), iron-deficiency anaemia, leukaemia, tuberculosis, and chronic vitamin (C and D) deficiencies are all considerations for differential diagnosis. Their diagnostic features are summarised in Table 3 and compared with the location and types of lesions identified on these elements. No fractures are observed on the extant remains; however, the absence of the majority of the skeletal elements means that trauma cannot be entirely discounted (Caffey, 1946, 1974).

4.1 | Frontal bone (FB0039, FB0040) and zygoma (FB0041)

Considered in isolation, the lesions on the fragmented frontal bone might accord with an aetiology of intra-cranial infection originating in the regions of greatest spiculation: the cone of the orbit, sinus and/or ethmoid. Intra-cranial infections in rare cases can develop suppurative complications, including meningitis and subdural empyema (Farmer & Wise, 1973; Skelton et al., 1992). Lesions are observed on the meninges as plaque-like deposits with capillary impressions and micropores, suggesting healing was underway at the time of death. Granulations associated with tubercular meningitis and lytic lesions characteristic of tuberculosis are not observed (Lewis, 2018, pp. 144, 156; Ortner, 2003, p. 94). Involvement of the skull is occasionally seen in cases of ICH which can recur past infancy in children of 2–4 years of age and beyond (Swerdloff et al., 1970). ICH can provoke deposition of pitted and layered new bone on the cranium, although most often affects the mandible, clavicle, ribs and long bones (Lewis, 2018, p. 145; Lewis & Gowland, 2009). The elements considered here do not present cortical hyperostosis.

The orbital roof lesions may suggest a metastasising secondary bone tumour, such as neuroblastoma. However, no osteoclastic activity is discerned, and the lesions do not present the "hair-on-end" appearance typical of metastatic deposits (Ortner, 2003, pp. 536–7). Bilateral diffuse microporosity across the orbital roof is consistent with grade 1 *cribra orbitalia* (Stuart-Macadam, 1985), the aetiology of which includes genetic and acquired anaemias, infectious disease, subperiosteal inflammation, and B_{12}/folate deficiency (Brickley, 2018; Oxenham & Cavill, 2010; Stuart-Macadam, 1992; Walker et al., 2009; Wapler et al., 2004). Similar to findings by Rivera and Lahr (2017), this individual presents no evidence of marrow hyperplasia, with cortical

TABLE 3 Differential diagnosis for non-adult elements

Aetiology	Diagnostic and characteristic features	Features present?	References
Intra-cranial infection	Localised sclerosis surrounding a central sequestrum	No	Ortner, 2003, pp. 192–194
Metastatic neuroblastoma	Metastases display hair-on-end appearance on the cranium and layered appearance on long bones and are often lytic	No	Ortner, 2003, pp. 536–537
Non-specific meningitis	Endocranial lesions surrounding the meninges. May be associated with epidural haematoma	Yes	Lewis, 2004; Schultz, 1993
	Chronic cases may be associated with osteopenia or disuse atrophy	No	Lewis, 2004
Infantile cortical hyperostosis (ICH)	Periosteal new bone deposition in individuals before 1 year of age. The condition may reoccur for several years with manifestations including interosseous bridging, mandibular asymmetry, radial head dislocation, and tibial bowing	No features of recurrent ICH are observed on the available elements	Aufderheide & Rodríguez-Martín, 1998, p. 364; Blank, 1975; Caffey & Silverman, 1945; Lewis, 2018, pp. 145–147; Ortner, 2003, p. 417; Rana et al., 2009;
	Woven periosteal new bone deposited in concentric layers, separated from the cortex. Lesions commonly on mandible, scapula, clavicle, ulna and ribs. Long bone lesions spare the epiphyses. Cortical thickness doubles or triples in size and the medullary cavity can widen. Cranial lesions may also result in thickened cortex and result in delayed fontanelle closure	No. Lesions represent reactive spicular bone growth. Cortical thickness is increased on the ulna, but the medullary cavity has not widened	
	In cases of multiple lesions, they are likely to be asymmetrical on the long bones	Uncertain. Lesions are symmetrical where they can be assessed	
	Affected bones may become osteoporotic	No	
Iron-deficiency anaemia	Porous hypertrophic cranial lesions, especially on the ectocranial surface of the frontal and parietal bones and orbital vaults, and occasionally on the zygomae. Resorption of the outer table, marrow hyperplasia and enlargement of the diploë are also common	Pitting in the orbital roofs alongside periosteal new bone deposition is present, but is not associated with resorption or marrow hyperplasia	Aksoy et al., 1966; Ortner, 2003, pp. 369–372; Stuart-Macadam, 1989, p. 215
	Post-cranial changes include osteoporosis, especially in the elbow, and coarse trabecular striations	No	
Leukaemia	Diffuse osteolytic lesions and porosity, enlargement of vascular foramina, and fine periosteal new bone especially on long bones and ribs. Can be associated with cortical resorption	No, the new bone deposition is not associated with any lytic lesions	Lewis, 2018, pp. 206–207; Ortner, 2003, p. 376
	Radiolucent band on metaphyseal side of growth plate	Metaphyses are absent	
	Generalised osteopenia	No	

(Continues)

TABLE 3 (Continued)

Aetiology	Diagnostic and characteristic features	Features present?	References
Tuberculosis	Cranial lesions in children commonly involve round lytic foci, sometimes with a sequestrum. Resorption of the inferior lateral orbital margin, maxilla, zygoma or mandibular angle may also be seen	No, there is no evidence of infection or resorption	Lewis, 2018, pp. 155–164; Ortner, 2003, pp. 227–263
	Granulomata in one or more joints, leading to necrosis. Long bone lesions marked by involucrum and sequestrum, with osteoporosis in affected limb/s	No	
	Vertebral body abscesses, lytic lesions and necrosis	Vertebrae are absent	
	Periosteal new bone and lytic lesions on the pleural surface of the ribs.	No. Lesions evident on pleural surfaces but are not lytic	
	Periosteal reactive bone (*spina ventosa*) on the tubular bones of the extremities	Extremities are absent	
Vitamin C deficiency (scurvy)	Porosity and/or periosteal new bone deposition on the cranium, usually bilateral because of subdural/subperiosteal haemorrhages: endocranial aspect of calvarium; ectocranial aspect of parietals and/or squamous temporals; sphenoid (greater wing, lesser wing, pterygoid plates, foramen rotundum); orbital vaults; zygomae (lateral and posterior); maxillae (anterior, posterior and palatal surfaces); occipital (inferior aspect of *pars basilaris)*	Yes. Porosity and new bone deposition on all extant cranial elements, including the frontal squama, orbits and zygoma	Brickley & Ives, 2006; Brickley & Ives, 2008, p. 57; Lewis, 2018, pp. 213–218; Ortner & Ericksen, 1997; Ortner et al., 1999; Ortner et al., 2001; Ortner, 2003, pp. 284–287; Snoddy et al., 2018
	Porosity and/or periosteal new bone deposition on mandible, usually bilateral because of subperiosteal haemorrhages: medial aspect; coronoid process; mylohyoid line; alveolar processes and sockets. Dentition may be loosening and/or lost ante-mortem and may exhibit enamel hypoplasia	Yes, periosteal lesions on the lateral and medial aspect of the rami and corpus. No evidence of AMTL	
	Porosity and/or periosteal new bone deposition on supraspinous and infraspinous fossae of scapulae	Scapulae are absent	
	Fracture and/or enlargement of ribs ("scorbutic rosary") adjacent to costochrondral junction. Periosteal new bone deposition on antero-lateral aspect of shaft	Yes, periosteal lesions observed on the pleural and external surfaces of the extant ribs	
	Porosity and/or new bone deposition on the pelvis, especially the visceral surface of the ilium	Pelvis is absent	
	New bone deposition on long bone metaphyses and diaphyses, especially because of bilateral ossified haematomata. Metaphyseal cupping/flaring	Yes, extensive new bone deposition on ulna with evidence of subperiosteal haematomata on diaphysis. Metaphyses absent	

TABLE 3 (Continued)

Aetiology	Diagnostic and characteristic features	Features present?	References
Vitamin D deficiency (rickets)	Delayed fontanelle closure. Craniotabes. Expansion of diploë and thinning of inner and outer tables. Frontal and parietal bossing. Spiculated new bone deposition and or/porosity on cranial vault and orbits	Spicular new bone deposition is observed on the cranium. Fontanelles are closed, therefore delay cannot be assessed	Brickley & Ives, 2008, pp. 103–105; Lewis, 2018, pp. 209–213; Mays et al., 2006; Ortner, 2003, pp. 393–398; Ortner & Mays, 1998
	Medial angulation of the mandibular ramus. Delayed eruption of dentition, enamel hypoplasia and caries	No. Dental eruption does not appear to be delayed	
	Vertebral body compression. Kyphosis or scoliosis, often of T9–L3	Vertebrae are absent	
	Alteration of rib neck angle. Abnormal flattening or curvature of the ribs. Enlargement and beading of costochrondral rib junction ("rachitic rosary"). Periosteal new bone deposition on anterior surface. Pigeon chest deformity	Extant portions of ribs are normal in morphology. New bone deposition is on the pleural and external surfaces, and the costochrondral junction is not present to assess	
	Abnormal curvature/concavity of ilium. Deformity due to delayed growth	Pelvis is absent	
	Flaring, cupping and fraying of long bone distal metaphyses. Bending deformities (*valgus* and *varus*), angulation of the femoral neck and/or knees. Periosteal new bone deposition mid-diaphysis. Generalised osteopenia, growth stunting, fractures, and cortical thinning or thickening may also be observed	Extant portion of ulna diaphysis displays no evidence of bending deformity, and distal metaphysis is not preserved. Cortical thickening is observed	

thinning and diploic expansion only observed in the regions of the most prolific lesions.

The active, disorganised periosteal new bone and microporosity in the orbital roofs indicates extensive subperiosteal bleeding following intraocular haematoma. Bilateral intraocular haematomas can be caused by micro-trauma as a result of scurvy (Sloan et al., 1999), as well as major head trauma. The proliferative lesion in the anterior cranial fossa is consistent with subdural haematoma which, alongside the healing plaque-like lesions occupying the frontal squama, suggests this individual experienced multiple episodes of vitamin C deficiency. Diffuse capillary impressions and porotic lesions across the frontal squama indicate an inflammatory response to extravasated blood (Brickley & Mays, 2019; Snoddy et al., 2018; Stark, 2014). Such extensive bleeding can lead to iron-deficiency anaemia, sometimes noted to be co-morbid with scurvy (Buckley, 2000; Clark et al., 2009; Fain, 2005). Furthermore, cranial vault and orbital roof porosity are associated with vitamin D deficiency (rickets) as a consequence of the failure of osteoid to mineralise (Mays et al., 2006; Ortner & Mays, 1998); when healing, mineralisation commences and may result in the presentation of spiculated new bone (Brickley & Ives, 2008, p. 103).

Woven bone on the zygoma is observed on locations associated with *Mm. masseter*, *temporalis*, *orbicularis occuli*, *zygomaticus minor* and *major*, as well as branches of numerous arteries implicated in the movement of the face and mouth, indicating extensive subperiosteal haematomata (Snoddy et al., 2018, p. 879). Snoddy et al. (2018, p. 887) deem bilateral haemorrhage in the orbital roof diagnostic of scurvy, subperiosteal new bone and porosity on the endocranial surface suggestive, and lesions on the antero-lateral and posterior aspect of the zygoma suggestive when bilateral. The contralateral zygoma is unobservable, but the expression and location of the lesions are highly consistent with a scorbutic aetiology.

4.2 | Mandible (FB0042)

Mandibular lesions are associated with many of the aetiologies previously discussed, including ICH, leukaemia, tuberculosis, rickets and

scurvy. The lack of cortical hyperostosis and layered subperiosteal new bone rules out ICH, while lytic destruction and pitting characteristic of leukaemia and tuberculosis is not observed (Imamura et al., 2004; Lewis, 2018, pp. 145, 206). The mandibular rami retain a normal morphology and no evidence of enamel hypoplasia or caries is recorded on the extant dentition. Bilateral concentrations of woven periosteal new bone on the lateral and medial aspects of the ascending ramus, between the mental foramen and mental eminence, and in the region of the mylohyoid groove, are characteristic of subperiosteal haematomata caused by micro-trauma of the facial muscles. These include *Mm. mentalis*, *masseter*, and the *medial* and *lateral pterygoid*, essential for movement of the lower lip, mastication, and speech. Bilateral deposits of subperiosteal new bone on the medial surface of the rami are diagnostic of scurvy (Snoddy et al., 2018, p. 890).

4.3 | Left rib (FB0043) and right rib (FB0044)

Lesions on the pleural surfaces of the extant ribs could indicate a respiratory infection (Davies-Barrett et al., 2019), although the lack of lytic lesions on the extant portions of the ribs is inconsistent with a diagnosis of tuberculosis (Ortner, 2003, pp. 246, 376). Subperiosteal new bone deposition on the ribs is occasionally noted in scorbutic non-adults (Buckley et al., 2014; Snoddy et al., 2017). On the external surface, this may be attributed to micro-trauma associated with movement involving the *Mm. serratus anterior* and *pectoralis major* (Snoddy et al., 2018, p. 880), while lesions on the pleural surface form as a result of subperiosteal haemorrhage following expansion and contraction of the lungs. When bilateral, rib lesions are suggestive of scurvy (Snoddy et al., 2018, p. 891).

4.4 | Ulna (FB0045)

The fragmented ulna presents the most severe example of proliferative new bone deposition alongside subperiosteal haematoma amongst the non-adult elements. Widespread subperiosteal new bone on long bone diaphyses and/or metaphyses are diagnostic of scurvy when present alongside cranial lesions (Brickley & Ives, 2008, p. 57; Snoddy et al., 2018, pp. 891–2). Snoddy et al. (2018, p. 892) note that long bone lesions due to scurvy are expected to be bilateral, but subperiosteal haemorrhage occurring following trauma is unlikely to be symmetrical (Stark, 2014, p. 19). New bone deposition on the extant element traverses several muscle attachment sites, including *Mm. flexor digitorum profundus*, *pronator quadratus*, *extensor carpi ulnaris*, and *extensor pollicis longus*. The fragmentation of the distal metaphysis means that diagnostic radiological features of scurvy cannot be assessed (Brickley & Ives, 2008, pp. 62–63; Lewis, 2018, p. 217). The extent of spiculated new bone on this ulna exceeds many cases of long bone lesions in scorbutic non-adults in the bioarchaeological literature (Brown & Ortner, 2011; Buckley et al., 2014; Geber & Murphy, 2012; Ortner et al., 2001; Snoddy et al., 2017). Klaus (2014) presents two cases of non-adult scurvy with proliferative long bone lesions and Fain (2005, p. 126) reports radiographic evidence of diaphyseal "sheathing" of long bones. The extant ulna presents a rarely-observed case of long bone diaphyseal periosteal reaction alongside cortical thickening which, given its severity of expression, likely indicates a chronic process.

5 | DISCUSSION

The distribution and expression of lesions indicates a probable case of chronic scurvy, perhaps also alongside vitamin D and iron deficiencies. If it is not accepted that all elements derive from the same individual, the cranial elements still present a possible case of scurvy (Snoddy et al., 2018). However, it is important to emphasise that, observed in cross-section through μCT, the character of the lesions on the rib and ulna fragments were similar to those on the cranial elements and mandible. In addition to lesions both suggestive and diagnostic of scurvy, we report lesions in locations which have received less attention in the palaeopathological literature to date. These include the bilateral proliferative lesions on the supero-lateral aspect of the supra-orbital margin, lesions on the anterior zygoma, bilateral woven bone and porosity on the anterior margin of the mylohyoid groove, within the mandibular foramen, and circumferential "frosted" spiculations on the ulna diaphysis. Similar mandibular lesions have previously been observed (see Brickley & Ives, 2006, p. 166; Brown & Ortner, 2011, p. 200) but do not demonstrate subperiosteal new bone extending as far inferiorly on the mylohyoid groove as the present example. This young child appears to have experienced a severe and chronic case of vitamin C deficiency, resulting in more proliferative lesions—especially on the zygoma and ulna—than many presented in the available bioarchaeological literature. Below, we consider the possible causes of scurvy in this individual, the presentation of co-morbid nutrient deficiencies, and the wider evidence of scurvy from the 5th–3rd millennia BC.

5.1 | Scurvy: Causes, consequences and co-morbidities

Vitamin C is a cofactor for several enzymes involved in collagen hydroxylation, and is therefore essential for the formation of collagen and osteoid (Fain, 2005). Adequate vitamin C intake is crucial to ensure continued normal bone growth, blood formation, immune function, and the metabolism of iron and folate (Jacob & Sotoudeh, 2002; Lipschitz et al., 1971; Popovich et al., 2009). As humans cannot synthesise ascorbic acid, it must be obtained solely through vitamin C-rich foods, especially fresh produce such as citrus fruits and dark green vegetables; protein-rich foods such as milk, fish and meat contain very little vitamin C (Brickley & Ives, 2008, pp. 41–4; Fain, 2005). The nutritional content of fresh produce is significantly reduced when foods are cooked (Fain, 2005), likewise when animal milk is pasteurised and heat-treated (Brickley & Ives, 2008, p. 45). The recommended daily intake of vitamin C for 1–3 year olds is 15 mg

(NIH 2020). It is thought that if the bodily pool of vitamin C reaches <300 mg, scorbutic symptoms can commence any time between 29 and 90 days (Brickley & Ives, 2008, p. 45) and 6–10 months after the onset of dietary deficiency (Jaffe, 1972).

The role of ascorbic acid as a co-factor in at least 15 enzymes means that chronic dietary deficiency can lead to the failure of multiple physiological functions and, if untreated, is fatal (Padayatty & Levine, 2016). As observed in clinical settings, the consequences of scurvy include behavioural and soft tissue changes with visible and painful effects: loss of appetite; failure to gain weight; fatigue; depression; irritability; weakness; gingival bleeding and swollen gums (eventually leading to periodontal disease and AMTL); pinpoint bleeding in the skin (petechiae) and/or bruising (purpura) (Fain, 2005; Hirschmann & Raugi, 1999). Perhaps most severe is the increased tendency for chronic bleeding in subperiosteal and joint spaces because of both normal muscular use and trauma. This causes intense joint and muscle pain, swelling and haematoma, and can lead to restricted mobility, reducing individuals to resting on their back in a "frog position," with their limbs semi-flexed and externally rotated (Popovich et al., 2009). The resumption of osteoblastic activity, in the form of periosteal new bone deposition, usually indicates the restoration of sufficient vitamin C to the diet. Lesions may still form if the dietary intake is less than the recommended intake, since diets are usually only completely deficient in vitamin C during starvation (Brickley & Mays, 2019, p. 533). Cortical porosity caused by capillary proliferation can be produced while in a totally vitamin C-deficient state.

Scurvy is often observed to be co-morbid with other micronutrient deficiencies, resulting in complicated disease presentation as each affects (and may inhibit) the pathophysiology of the other. Importantly for this discussion, the biology of vitamin C, D and iron absorption and function are linked. As discussed above, extensive bleeding in chronic scurvy because of the weakening of blood vessel walls may exacerbate or lead to iron-deficiency anaemia, which can in turn inhibit the intestinal absorption of minerals, potentially exacerbating or causing rickets (Fain, 2005; Brickley & Ives, 2008, p. 113). As is clear from Table 3, many osseous characteristics of scurvy and rickets present similarly, especially on the costochondral junction of the rib and on long bone metaphyses, regions which are not available to observe for this individual. The presentation of both scurvy and rickets, when they co-occur, depends on the order in which they each develop, their healing status, and severity, and one disease usually dominates the other (Schattmann et al., 2016). Clinical research has observed that, in infants, the skeletal features of scurvy are more likely to be observable and may mask those of rickets (Bromer & Harvey, 1948; Cheadle, 1878). Bioarchaeological research into their co-occurrence has shown that rickets may be identified radiographically or microscopically, while scurvy is clearer to observe macroscopically (Schattmann et al., 2016). At the very least, the spiculated periosteal new bone observed on the ectocranial surface and orbital roofs of this individual are observed in cases of both scurvy and rickets and may suggest that nutritional co-morbidities were experienced by this child.

Given the young age of this individual, we must consider whether vitamin C deficiency resulted from direct dietary insufficiency, perhaps because of a lack of dietary diversity or seasonal/cyclical famine (Brickley, 2000), or from complications associated with breastfeeding or weaning. Additionally, vitamin D is mostly synthesised through exposure of the skin to UVB rays, with natural dietary sources mostly limited to eggs and oily fish (Brickley & Ives, 2008, p. 83; Holick, 2003). Although human breastmilk is high in vitamin C (Grewar, 1965), breastfeeding almost doubles the daily metabolic requirements for adults, to approximately 120 mg (NIH 2020). If this child was breastfed by a vitamin C-deficient individual, their intake would be significantly reduced. In contrast, breastmilk is low in vitamin D, and it is therefore essential that breastfeeding individuals maintain healthy levels of vitamin D through exposure to sunlight (Pettifor, 2004). The process of weaning can result in micro-nutrient deficiencies if the weaning diet is not carefully balanced (Davies & O'Hare, 2004; Tontisirin et al., 2002). Crucial for a nutritious weaning diet are the availability of appropriate substitute animal-based dairy products and dietary diversity (Iannotti & Lesorogol, 2014; Scrimshaw, 2003). Cereal-rich diets can lead to reduced calcium intake as cereal phytates bind to calcium, and the resulting imbalance affects vitamin D synthesis (Pettifor, 2004). Scarcity of dairy products and other staple foods, as well as an over-reliance on cereals, has rapid adverse effects on the diet and health of vulnerable individuals.

5.2 | Scurvy in prehistory

In a brief review of the literature, focussed mostly on the regions surrounding the Maltese islands, namely Europe and Africa, we found that prehistoric cases of scurvy are not reported as commonly as might be expected. This may be because osseous lesions are thought to develop only in response to a periodic or chronic lack of vitamin C intake (Crandall & Klaus, 2014). Until recently, identification of prehistoric cases of non-adult scurvy was largely hampered by two main issues: (i) the difficulties associated with distinguishing pathological new bone deposition from normal growth processes and (ii) the common practice of collective deposition across much of Europe and beyond from the second half of the 5th millennium BC, resulting in fragmented remains and incomplete skeletons which were often overlooked by traditional palaeopathological analyses. The exception to this are the numerous cases of prehistoric scurvy in the Americas identified by Ortner and colleagues through exhaustive analyses of museum collections of crania (Ortner et al., 2001, 1999). Increased bioarchaeological analyses of commingled assemblages in the past two decades has revealed the presence of chronic nutritional deficiencies, including of vitamin C, at apparently low prevalence rates in many regions from the Neolithic to the Early Bronze Age (Table 4).

Most identified cases in the literature present scurvy in neonates and infants. This is particularly so in the review of palaeopathological lesions from several early Neolithic chambered tombs and long barrows in Britain and Orkney where possible or probable cases of scurvy

TABLE 4 Scurvy in non-adults and adults from Neolithic to Early Bronze Age contexts

Site	Period	Evidence	Reference
Basta, Jordan	PPNB, 7550–5040 cal BC	"at least one or possibly two children", but diagnostic evidence not presented	Schultz, 1987
Hódmezővásárhely–Gorzsa, Hungary	Early Neolithic, 5950–5400 BC	Neonate: diffuse porosity on the cranium, mandible, scapulae, claviculae and long bones, alongside *cribra orbitalia*. Infant (6 months): porosity and proliferative new bone deposition on the cranium, scapulae and long bones	Masson, 2014
Nag-el-Carmila, Egypt	Predynastic, 3800–3600 BC	Infant (1 year±4 months): diffuse bilateral subperiosteal lesions on cranial elements, humeri, radii and femora	Pitre et al., 2016
Alepotrypa Cave, Greece	Late Neolithic, 5000–3200 BC	9 non-adults and 36 adults with porotic hyperostosis and *cribra orbitalia*, some of which may be attributed to scurvy, possibly co-morbid with anaemia, although no diagnostic evidence is presented	Papathanasiou, 2005
El Portalón, Spain	Chalcolithic, 3080–3070 BC	Child (6–7 years): two periods of growth interruption (1–3 years and 3–5 years), the latter of which was suggested to be the result of scurvy. Porosity on ectocranial surface, sphenoid, palate, maxillary alveoli, mandible. *Cribra orbitalia* in left orbit.	Castilla et al., 2014
West Tump long barrow, England	Early Neolithic, 3770–3630 BC	Infant: new bone deposition on orbital roof	Smith & Brickley, 2009, pp. 120–121
Fromefield long barrow, England	Early Neolithic	Neonate: new bone deposition on the palate and extensive postcranial porosity	Cuthbert, 2019, p. 117
Belas Knap long barrow, England	Early Neolithic, 3900–3500 BC	Infant: new bone deposition on orbital roof	Cuthbert, 2019, p. 113
Hazleton North long barrow, England	Early Neolithic, 3695–3620 cal BC	Two infants and two children. Infant 1: porosity and new bone in orbital roof. Infant 2 (9 months): porosity across maxilla and internal surface of mandible. Child 1 (5–6 years): porosity on ectocranial surface of frontal bone, palate, and orbit. Child 2 (8 years): bilateral orbital roof porosity; porosity on temporal bone and sphenoid	Cuthbert, 2019, pp. 113–5
Isbister ("Tomb of the Eagles"), South Ronaldsay, Orkney	Early Neolithic, 3380–2835 cal BC	Neonate with diffuse postcranial periosteal lesions. At least 4 older children and 15 adults present porosity on the greater wing of the sphenoid.	Lawrence, 2012
Barrow Clump, England	Early Bronze Age, 2200–1970 cal BC	Child (2 years): porosity and new bone deposition on endo- and ecto-cranial surfaces, porosity on sphenoid, new bone deposition on orbital roofs, porosity on maxilla and mandible, woven bone on left tibia	Mays, 2008

TABLE 4 (Continued)

Site	Period	Evidence	Reference
Quiani 7, South America	Early Formative Period, 1650–1250 BC	T15 (32–36 weeks prenatal weeks): porous new bone on sphenoid, mandible long bones and ilia, and thick new bone on all ribs, craniotabes, possible osteopenia T17 (F, 20–34 years): porosity and new bone on maxillae, sphenoid, orbital roofs and interior mandible. T17a (40 prenatal weeks): porous new bone in orbital roofs, lateral mandible, sphenoid, scapulae, endocranial surface of cranial elements, thick new bone on lateral shafts of ribs, porous new bone on all long bone diaphyses and ilia, possible osteopenia. T18 (38–40 prenatal weeks): porous new bone on endocranial surface of parietal, lateral and anterior mandible, scapulae, thick new bone on lateral shafts of ribs, porous new bone on all long bone diaphyses, possible osteopenia T19 (1.5 months): porous new bone on sphenoid, right orbital roof, microporosity on maxillae, thick new bone on lateral shafts of ribs, porous new bone on all long bone diaphyses, endochondral porosity, craniotabes, porotic hyperostosis, possible osteopenia	Snoddy et al., 2017

have recently come to light (Cuthbert, 2019; Lawrence, 2012). However, the apparently greater prevalence of scurvy in Neolithic Orkney, including in possibly more than a dozen adults, may be attributed to difficulties in obtaining adequate nutrition on a seasonal basis on the islands, as well as poor weaning foods and undernourished pregnant and/or nursing individuals (Lawrence, 2012, p. 539). Similar conclusions were reached for the high prevalence of scurvy in perinates at the site of Quiani 7 in the Atacama desert, where nutritious foods may have been periodically scarce during the agricultural transition (Snoddy et al., 2017).

5.3 | The Maltese context

The above review reveals an apparent lack of scurvy in the prehistoric central Mediterranean. This young child from the Xagħra Circle may therefore currently represent the earliest probable case of scurvy in this region. In the context of prehistoric Malta, infants and children may have been weaned onto diets which were low in dairy or contained non-fermented dairy products. Zooarchaeological finds of relatively large numbers of young sheep from prehistoric sites in Malta suggest dairying was an important part of the economy, but the availability and distribution of dairy cannot be ascertained (McLaughlin et al., 2020). It is quite probable that the Neolithic population experienced periodic scarcity of fresh fruits and vegetables, for example on a seasonal basis, and were heavily reliant on cereal foods. The young age of the child, the extent of skeletal lesions, and the evidence for mixed healing stages lead us to hypothesise that they either experienced chronic, recurrent vitamin C deficiency, or a consistently low dietary intake. Rickets, if present, may have been a late onset in this child, perhaps as they became too ill to move freely and spend time outside.

Chronologically, the context within which this individual was deposited aligns with the declining phase of the "Temple culture." Wider palaeoenvironmental evidence indicates increased aridification and soil erosion from the mid-late third millennium BC (French et al., 2018). The archaeobotanical and zooarchaeological evidence do not indicate specific incidences of resource stress or famine (McLaughlin et al., 2020), although dietary isotopic evidence reveals decreasing $\delta^{15}N$ over time (McLaughlin et al., in press). Other indicators of nutritional and environmental stress, such as *cribra orbitalia*, porotic hyperostosis and enamel hypoplasia, are markedly low in incidence and prevalence across the excavated population from the Circle, although incidences of enamel hypoplasia increase from 2500 cal BC onwards (Power et al., in press b; Stoddart et al., 2009a). The apparently unique nature of these lesions precludes population level inferences. However, it is axiomatic that infant and child mortality and morbidity provide insight into overall population health by virtue of their physiological sensitivity (Hewlett, 1991; Lewis, 2007; Power, 2012; Saunders & Barrans, 1999). This child may signal an

increasingly unstable livelihood for the Gozitan population during the final stages of the remarkably resilient "Temple culture."

Beyond the insights these diagnoses provide regarding physiological, dietary and palaeoenvironmental conditions in mid-third millennium BC Gozo, the spatial proximity of these elements within the dense deposit of the Shrine area is striking. Taphonomic analysis provided evidence for the redistribution of remains throughout the Circle hypogeum (Stoddart et al., 2009a; Thompson, 2020; Thompson et al., in press) and clusters of similar elements were noted during excavation, such as groups of crania, loose teeth, and long bones in the Deep Zone (Stoddart et al., 2009b, p. 137). Given these indicators for the grouping of elements, it is possible that the visible difference of these pathological elements was acknowledged, leading to their careful placement near to each other when redistributed following initial deposition.

6 | CONCLUSIONS

The aim of this study was to combine macroscopic and radiological analyses of periosteal lesions on disarticulated remains to both ascertain the number of individuals represented and provide a differential diagnosis. The disarticulated remains were deposited in a discrete 1 × 1-m deposit in the Xagħra Circle hypogeum and, upon analysis, proved to be consistent in age, likely deriving from a single individual of 2–4 years old at death. Macroscopic and radiological analyses of the lesions across the extant elements were observed to be largely consistent in character, including raised and spiculated new bone deposits indicating subperiosteal haematomata in both orbital roofs and on the distal ulna, and healing lesions incorporating microporosity on the endocranial surface, posterior aspect of the zygoma, mandibular corpus, and both extant ribs. Given the distribution and character of the lesions, this young child experienced chronic scurvy, possibly co-morbid with rickets and/or iron-deficiency anaemia, and represents an early case of this disease in the Mediterranean region. In context, this finding may fit into an already-identified pattern of declining population health during the late third millennium BC in Malta, but may also signal an individual case of poor childhood health or neglect.

This study highlights the importance of implementing palaeopathological analyses on commingled and disarticulated material. The integration of macroscopic analyses and μCT imaging supports recent appeals for multiple scales of observation to further the dialogue between palaeopathological and clinical studies (Stark, 2014). In this case, we have presented details of radiological observations which may be associated with scurvy on the extant cranial and post-cranial remains from this individual. As has been previously noted, the diagnostic radiological signs of scurvy are located in the area of the metaphyses and epiphyses, which are often not observable on archaeological remains as a result of poor preservation (Brickley & Mays, 2019). Such an approach can, as we have demonstrated, lead to the posthumous re-unification of individuals, while recording lesion presence and incidence levels even in commingled deposits can shed light on the experience of health, disease and care in the past. Further research is warranted to contextualise the evidence presented here, and we hope that our approach leads to renewed efforts to analyse population health from contemporary commingled assemblages in the central Mediterranean region.

ACKNOWLEDGEMENTS

We are grateful to Sharon Sultana at Heritage Malta and Anthony Pace (former Superintendent) at the Superintendence of Cultural Heritage Malta for access to the Xagħra Circle assemblage and permission to transport these remains from Malta for micro-CT scanning at the Cambridge Biotomography Centre. We acknowledge the resources provided by the Cambridge Biotomography Centre and Macquarie Medical Imaging. We are thankful to anonymous peer reviewers for their helpful comments on a previous version of this paper; any errors remain our own. This research was carried out during Jess Thompson's PhD, funded by the Arts and Humanities Research Council and supported by the Archaeology and Anthropology Fund, Magdalene College, University of Cambridge, as part of the *Fragility and Sustainability in Restricted Island Environments* Project (FRAGSUS: www.qub.ac.uk/sites/FRAGSUS). FRAGSUS was funded by an Advanced Investigator Grant (323727) from the European Research Council and led by Caroline Malone.

CONFLICT OF INTEREST

The authors declare no known conflict of interest.

AUTHOR CONTRIBUTIONS

Jess E. Thompson: Conceptualization; formal analysis; funding acquisition; writing-original draft; writing-review and editing. **Ronika K. Power:** Conceptualization; supervision; formal analysis; writing-original draft; writing-review and editing. **Bernadette Mercieca-Spiteri:** Supervision; resources; writing-review and editing. **John S. Magnussen:** Formal analysis; data curation; resources; writing-review and editing. **Margery Pardey:** Data curation; resources; writing-review and editing. **Laura T. Buck:** Resources; data curation; writing-review and editing. **Jay T. Stock:** Resources; writing-review and editing. **T. Rowan McLaughlin:** Formal analysis; writing-review and editing. **Simon Stoddart:** Supervision; writing-review and editing. **Caroline Malone:** Funding acquisition; supervision; writing-review and editing.

DATA AVAILABILITY STATEMENT

The data that support the findings of this study are available on request from the corresponding author, with permission of Heritage Malta and the Superintendence of Cultural Heritage Malta.

ORCID

Jess E. Thompson https://orcid.org/0000-0002-9389-0545
Ronika K. Power https://orcid.org/0000-0002-1092-8131
John S. Magnussen https://orcid.org/0000-0002-4422-276X

Margery Pardey https://orcid.org/0000-0002-5675-7606
Laura T. Buck https://orcid.org/0000-0002-1768-9049
Jay T. Stock https://orcid.org/0000-0003-0147-8631
T. Rowan McLaughlin https://orcid.org/0000-0003-4923-1339
Simon Stoddart https://orcid.org/0000-0002-5480-7075
Caroline Malone https://orcid.org/0000-0002-7710-0013

REFERENCES

Aksoy, M., Camil, N., & Erdem, S. (1966). Roentgenographic bone changes in chronic iron deficiency anemia. *Blood*, *27*, 677–686.

AlQahtani, S. J., Hector, M. P., & Liversidge, H. M. (2010). Brief communication: The London atlas of human tooth development and eruption. *American Journal of Physical Anthropology*, *142*(3), 481–490. https://doi.org/10.1002/ajpa.21258

Aufderheide, A. C., & Rodríguez-Martín, C. (1998). *The Cambridge encyclopaedia of human paleopathology*. Cambridge University Press.

Barratt, R., Malone, C., McLaughlin, R., & Parkinson, E. (2020). Hypogea and the clubhouse: Neolithic Malta's houses of the living and houses of the dead. In A. Barclay, D. Field, & J. Leary (Eds.), *Houses of the dead?* (p. 15, 38). Oxbow Books.

Blank, E. (1975). Recurrent Caffey's cortical hyperostosis and persistent deformity. *Pediatrics*, *55*(6), 856–860.

Brant, W. E., & Helms, C. (2012). *Fundamentals of diagnostic radiology (4th Editio)*. Lippincott, Williams and Wilkins.

Brickley, M., & Ives, R. (2006). Skeletal manifestations of infantile scurvy. *American Journal of Physical Anthropology*, *129*, 163–172.

Brickley, M., & Ives, R. (2008). *The bioarchaeology of metabolic bone disease*. Elsevier.

Brickley, M. B. (2018). *Cribra orbitalia* and porotic hyperostosis: A biological approach to diagnosis. *American Journal of Physical Anthropology*, *167*(4), 896–902. https://doi.org/10.1002/ajpa.23701

Brickley, M. B., & Mays, S. (2019). Metabolic disease. In J. E. Buikstra (Ed.), *Ortner's identification of pathological conditions in human skeletal remains (Third Edit)* (pp. 531–566). Academic Press.

Bromer, R. S., & Harvey, R. M. (1948). The roentgen diagnosis of rickets associated with other skeletal diseases of infants and children. *Radiology*, *51*(1), 1–10. https://doi.org/10.1148/51.1.1

Brown, M., & Ortner, D. J. (2011). Childhood scurvy in a medieval burial from Mačvanska Mitrovica, Serbia. *International Journal of Osteoarchaeology*, *21*(2), 197–207. https://doi.org/10.1002/oa.1124

Buckley, H. R., Kinaston, R., Halcrow, S. E., Foster, A., Spriggs, M., & Bedford, S. (2014). Scurvy in a tropical paradise? Evaluating the possibility of infant and adult vitamin C deficiency in the Lapita skeletal sample of Teouma, Vanuatu, Pacific islands. *International Journal of Paleopathology*, *5*, 72–85.

Buckley, H. R. (2000). Subadult health and disease in prehistoric Tonga, Polynesia. *American Journal of Physical Anthropology*, *113*(4), 481–505. https://doi.org/10.1002/1096-8644(200012)113:4%3C481::AID-AJPA4%3C3.0.CO;2-1

Buikstra, J. E., & Ubelaker, D. H. (1994). *Standards for data collection from human skeletal remains* (p. 44). Arkansas Archaeological Survey Research Series No.

Caffey, J. (1946). Multiple fractures in the long bones of infants suffering from chronic subdural hematoma. *American Journal of Roentgenology*, *56*(2), 163–173. https://doi.org/10.1007/s11999-010-1666-0

Caffey, J. (1974). The whiplash shaken infant syndrome: Manual shaking by the extremities with whiplash-induced intracranial and intraocular bleedings, linked with residual permanent brain damage and mental retardation. *Pediatrics*, *54*(4), 396–403.

Caffey, J., & Silverman, W. A. (1945). Infantile cortical hyperostosis. Preliminary report on a new syndrome. *American Journal of Roentgenology and Radium Therapy*, *54*(1), 1–16.

Castilla, M., Carretero, J.-M., Gracia, A., & Arsuage, J.-L. (2014). Evidence of rickets and/or scurvy in a complete Chalcolithic child skeleton from the El Portalón site (Sierra de Atapuerca, Spain). *Journal of Anthropological Sciences: Reports*, *92*, 257–271. https://doi.org/10.4436/JASS.92005

Cheadle, W. B. (1878). On three cases of scurvy supervening on rickets in young children. *The Lancet*, *112*(2881), 685–687. https://doi.org/10.1016/S0140-6736(02)43922-0

Clark, N. G., Sheard, N. F., & Kelleher, J. F. (2009). Treatment of iron-deficiency anemia complicated by scurvy and folic acid deficiency. *Nutrition Reviews*, *50*(5), 134–137. https://doi.org/10.1111/j.1753-4887.1992.tb01304.x

Crandall, J. J., & Klaus, H. D. (2014). Advancements, challenges, and prospects in the paleopathology of scurvy: Current perspectives on vitamin C deficiency in human skeletal remains. *International Journal of Paleopathology*, *5*, 1–8. https://doi.org/10.1016/J.IJPP.2014.04.005

Cunha, E. (2006). Pathology as a Factor of Personal Identity in Forensic Anthropology. In A. Schmitt, E. Cunha, & J. Pinheiro (Eds.), *Forensic anthropology and medicine: completementary sciences from recovery to cause of death* (pp. 333–358). Humana Press.

Cuthbert, G. S. (2019). *Enriching the Neolithic: The forgotten people of the barrows*. University of Exeter.

Davies, D. P., & O'Hare, B. (2004). Weaning: A worry as old as time. *Current Paediatrics*, *14*(2), 83–96. https://doi.org/10.1016/j.cupe.2003.11.006

Davies-Barrett, A. M., Antoine, D., & Roberts, C. A. (2019). Inflammatory periosteal reaction on ribs associated with lower respiratory tract disease: A method for recording prevalence from sites with differing preservation. *American Journal of Physical Anthropology*, *168*(3), 530–542. https://doi.org/10.1002/ajpa.23769

Fain, O. (2005). Musculoskeletal manifestations of scurvy. *Joint Bone Spine*, *72*(2), 124–128. https://doi.org/10.1016/j.jbspin.2004.01.007

Farmer, T. W., & Wise, G. R. (1973). Subdural empyema in infants, children and adults. *Neurology*, *23*(3), 254–254. https://doi.org/10.1212/WNL.23.3.254

Fedorov, A., Beichel, R., Kalpathy-Cramer, J., Finet, J., Fillion-Robin, J.-C., Pujol, S., … Kikinis, R. (2012). 3D slicer as an image computing platform for the quantitative imaging network. *Magnetic Resonance Imaging*, *30*(9), 1323–1341. Retrieved from. http://www.slicer.org

French, C., Taylor, S., McLaughlin, R., Cresswell, A., Kinnaird, T., Sanderson, D., … Malone, C. (2018). A Neolithic palaeo-catena for the Xagħra Upper Coralline Limestone plateau of Gozo, Malta, and its implications for past soil development and land use. *Catena*, *171*, 337–358. https://doi.org/10.1016/j.catena.2018.07.039

Geber, J., & Murphy, E. (2012). Scurvy in the Great Irish Famine: Evidence of vitamin C deficiency from a mid-19th century skeletal population. *American Journal of Physical Anthropology*, *148*(4), 512–524. https://doi.org/10.1002/ajpa.22066

González-Reimers, E., Trujillo-Mederos, A., Machado-Calvo, M., Castañeyra-Ruiz, M., Ordóñez, A. C., & Arnay-de-la-Rosa, M. (2015). A skeletal case of hypertrophic osteoarthropathy from the Canary Islands dating from 1000 BP. *International Journal of Paleopathology*, *11*, 1–6. https://doi.org/10.1016/j.ijpp.2015.07.001

Grewar, D. (1965). Infantile scurvy. *Clinical Pediatrics*, *4*, 82–89.

Hewlett, B. S. (1991). Demography and childcare in preindustrial societies. *Journal of Anthropological Research*, *47*, 1–37. https://doi.org/10.1086/jar.47.1.3630579

Hirschmann, J. V., & Raugi, G. J. (1999). Adult scurvy. *Journal of the American Academy of Dermatology*, *41*(6), 895–906. https://doi.org/10.1016/s0190-9622(99)70244-6

Holick, M. F. (2003). Vitamin D: A millenium perspective. *Journal of Cellular Biochemistry*, *88*(2), 296–307. https://doi.org/10.1002/jcb.10338

Iannotti, L., & Lesorogol, C. (2014). Dietary intakes and micronutrient adequacy related to the changing livelihoods of two pastoralist

communities in Samburu, Kenya. *Current Anthropology*, *55*(4), 475–482. https://doi.org/10.1086/677107

Imamura, M., Kakihara, T., Yamamoto, K., Imai, C., Tanaka, A., & Uchiyama, M. (2004). Primary tuberculous osteomyelitis of the mandible. *Pediatrics International*, *46*(6), 736–739. https://doi.org/10.1111/j.1442-200x.2004.01992.x

Jaffe, H. L. (1972). *Metabolic, degenerative, and inflammatory diseases of bones and joints*. Lea and Febiger.

Jones, E. (1998). Skeletal growth and development as related to trauma. In N. E. Green & M. F. Swiontkowski (Eds.), *Skeletal trauma in children* (pp. 1–16). W.B. Saunders Company.

Klaus, H. D. (2014). Subadult scurvy in Andean South America: Evidence of vitamin C deficiency in the late pre-Hispanic and Colonial Lambayeque Valley, Peru. *International Journal of Paleopathology*, *5*, 34–45. https://doi.org/10.1016/j.ijpp.2013.09.002

Lawrence, D. M. (2012). *Orkney's first farmers: Reconstructing biographies from osteological analysis to gain insights into life and society in a Neolithic community on the edge of Atlantic Europe*. University of Bradford.

Lewis, M. (2004). Endocranial lesions in non-adult skeletons: Understanding their aetiology. *International Journal of Osteoarchaeology*, *14*, 82–97.

Lewis, M. (2007). *The bioarchaeology of children: Perspectives from biological and forensic anthropology*. Cambridge University Press.

Lewis, M. (2018). *Palaeopathology of children. Identification of pathological conditions in the human skeletal remains of non-adults*. Academic Press.

Lewis, M., & Gowland, R. (2009). Infantile Cortical Hyperostosis: cases, causes and contridictions. In M. Lewis & M. Clegg (Eds.), *Proceedings of the ninth annual conference of the british association for biological anthropology and osteoarchaeology* (pp. 43–51). Archaeopress BAR International Series 1981.

Lipschitz, D. A., Bothwell, T. H., Seftel, H. C., Wapnick, A. A., & Charlton, R. W. (1971). The role of ascorbic acid in the metabolism of storage iron. *British Journal of Haematology*, *20*(2), 155–163. https://doi.org/10.1111/j.1365-2141.1971.tb07024.x

Malone, C., Cutajar, N., McLaughlin, T. R., Mercieca-Spiteri, B., Pace, A., Power, R. K., … Whittle, A. (2019). Island questions: the chronology of the Brochtorff Circle at Xagħra, Gozo, and its significance for the Neolithic sequence on Malta. *Archaeological and Anthropological Sciences*, *11*(8), 4251–4306. https://doi.org/10.1007/s12520-019-00790-y

Malone, C., Stoddart, S., Trump, D., Bonanno, A., Gouder, T., & Pace, A. (2009). *Mortuary customs in prehistoric Malta: Excavations at the Brochtorff Circle at Xagħra (1987–1994)*. McDonald Institute for Archaeological Research.

Mann, R. W., & Hunt, D. R. (2012). *Photographic regional atlas of bone disease: A guide to pathologic and normal variation in the human skeleton*. Charles C Thomas Ltd.

Masson, M. (2014). The osteological evidence of Neolithic populations from the Southern Great Plain of Hungary (Szegedi Tudományegyetem). *Szegedi Tudományegyetem*, *Szeged*, *Hungary*.. https://doi.org/10.14232/phd.2218

Mays, S. (2008). A likely case of scurvy from early bronze age Britain. *International Journal of Osteoarchaeology*, *18*(2), 178–187. https://doi.org/10.1002/oa.930

Mays, S., Brickley, M., & Ives, R. (2006). Skeletal manifestations of rickets in infants and young children in a historic population from England. *American Journal of Physical Anthropology*, *129*(3), 362–374. https://doi.org/10.1002/ajpa.20292

McLaughlin, R., McCormick, F., Hamilton-Dyer, S., Bates, J., Morales-Mateos, J., French, C., Chatzimpaloglou, P., … Malone, C. (2020). Economy, environment and resources in prehistoric Malta. In C. Malone, R. Grima, R. McLaughlin, E. Parkinson, S. Stoddart, & N. Vella (Eds.), *Temple places: Excavating cultural sustainability in prehistoric Malta* (pp. 281–307). McDonald Institute for Archaeological Research.

McLaughlin, R., Power, R. K., Mercieca-Spiteri, B., Parkinson, E., Lightfoot, E., Varalli, A., Thompson, J. E., … Malone, C. (in press). An isotopic study of palaeodiet at Xagħra and Xemxija. In S. Stoddart, R. K. Power, J. E. Thompson, B. Mercieca-Spiteri, R. McLaughlin, A. Pace, & C. Malone (Eds.), *Temple P*. McDonald Institute for Archaeological Research.

Mercieca-Spiteri, B., Power, R. K., Parkinson, E., Thompson, J. E., O'Connell, T., & Stock, J. (in press). New approaches to the bioarchaeology of complex multiple interments. In S. Stoddart, R. K. Power, J. E. Thompson, B. Mercieca-Spiteri, R. McLaughlin, A. Pace, & C. Malone (Eds.), *Temple people: Bioarchaeology, resilience and culture in prehistoric Malta*. McDonald Institute for Archaeological Research.

Ortner, D. J. (2003). *Identification of pathological conditions in human skeletal remains*. Academic Press.

Ortner, D. J., Butler, W., Cafarella, J., & Milligan, L. (2001). Evidence of probable scurvy in subadults from archeological sites in North America. *American Journal of Physical Anthropology*, *114*(4), 343–351. https://doi.org/10.1002/ajpa.1046

Ortner, D. J., & Ericksen, M. F. (1997). Bone changes in the human skull probably resulting from scurvy in infancy and childhood. *International Journal of Osteoarchaeology*, *7*(3), 212–220. https://doi.org/10.1002/(sici)1099-1212(199705)7:3%3C212::aid-oa346%3E3.0.co;2-5

Ortner, D. J., Kimmerle, E. H., & Diez, M. (1999). Probable evidence of scurvy in subadults from archeological sites in Peru. *American Journal of Physical Anthropology*, *108*(3), 321–331. https://doi.org/10.1002/(SICI)1096-8644(199903)108:3%3C321::AID-AJPA7%3E3.0.CO;2-7

Ortner, D. J., & Mays, S. (1998). Dry-bone manifestations of rickets in infancy and early childhood. *International Journal of Osteoarchaeology*, *8*(1), 45–55. https://doi.org/10.1002/(SICI)1099-1212(199801/02)8:1%3C45::AID-OA405%3E3.0.CO;2-D

Oxenham, M. F., & Cavill, I. (2010). Porotic hyperostosis and cribra orbitalia: the erythropoietic response to iron-deficiency anaemia. *Anthropological Science*, *118*(3), 119–200. https://doi.org/10.1537/ase.100302

Padayatty, S. J., & Levine, M. (2016). Vitamin C: the known and the unknown and Goldilocks. *Oral Diseases*, *22*, 463–493. https://doi.org/10.1111/odi.12446

Papathanasiou, A. (2005). Health status of the Neolithic population of Alepotrypa Cave, Greece. *American Journal of Physical Anthropology*, *126*, 377–390. https://doi.org/10.1002/ajpa.20140

Pettifor, J. M. (2004). Nutritional rickets: Deficiency of vitamin D, calcium, or both? *The American Journal of Clinical Nutrition*, *80*(6), 1725S–1729S. https://doi.org/10.1093/ajcn/80.6.1725S

Pinheiro, J., Cunha, E., Cordeiro, C., & Vieira, D. N. (2004). Bridging the gap between forensic anthropology and osteoarchaeology: A case of vascular pathology. *International Journal of Osteoarchaeology*, *14*, 137–144. https://doi.org/10.1002/oa.718

Pitre, M. C., Stark, R. J., & Gatto, M. C. (2016). First probable case of scurvy in ancient Egypt at Nag el-Qarmila, Aswan. *International Journal of Paleopathology*, *13*(11–19), 11–19. https://doi.org/10.1016/j.ijpp.2015.12.003

Popovich, D., McAlhany, A., Adewumi, A. O., & Barnes, M. M. (2009). Scurvy: Forgotten but definitely not gone. *Journal of Pediatric Health Care*, *23*(6), 405–415. https://doi.org/10.1016/j.pedhc.2008.10.008

Power, R. K. (2012). *From the cradle to the grave: Child, infant and foetal burials in the Egyptian archaeological record from the Early Dynastic Period to the Middle Kingdom (ca. 3300–1650 BC)*. Macquarie University.

Power, R. K., Mercieca-Spiteri, B., McLaughlin, R., Thompson, J. E., Carruthers, J., Massingham, S., … Magnussen, J. (in press b). Dental pathology in the Xagħra Hypogeum: Oral health, activity and intervention in Neolithic Malta. In S. Stoddart, R. K. Power, J. E. Thompson, B. Mercieca-Spiteri, R. McLaughlin, A. Pace, & C. Malone (Eds.), *Temple people: Bioarchaeology, resilience and culture in Prehistoric Malta*. McDonald Institute for Archaeological Research.

Power, R. K., Mercieca-Spiteri, B., Thompson, J. E., McLaughlin, R., Carruthers, J., Vogel, H., … Magnussen, J. (in press a). General pathology in the Xagħra Hypogeum: Biocultural insights into population health, trauma and care in Neolithic Malta. In S. Stoddart, R. K. Power, J. E. Thompson, B. Mercieca-Spiteri, T. R. McLaughlin, A. Pace, & C. Malone (Eds.), *Temple people: Bioarchaeology, resilience and culture in prehistoric Malta*. McDonald Institute for Archaeological Research.

Rana, R. S., Wu, J. S., & Eisenberg, R. L. (2009). Periosteal reaction. *American Journal of Roentgenology*, *193*(4), W259–W272. https://doi.org/10.2214/AJR.09.3300

Richardson, M. (2001). *Online musculoskeletal radiology book*. University of Washington. Retrieved from. https://rad.washington.edu/about-us/academic-sections/musculoskeletal-radiology/teaching-materials/online-musculoskeletal-radiology-book/

Rittemard, C., Colombo, A., Desbarats, P., Dutailly, B., Dutour, O., & Coqueugniot, H. (2019). The periosteum dilemma in bioarcheology: Normal growth or pathological condition?—3D discriminating microscopic approach. *Journal of Archaeological Science: Reports*, *24*, 236–243. https://doi.org/10.1016/j.jasrep.2018.12.012

Rivera, F., & Lahr, M. M. (2017). New evidence suggesting a dissociated etiology for *cribra orbitalia* and porotic hyperostosis. *American Journal of Physical Anthropology*, *164*(1), 76–96. https://doi.org/10.1002/ajpa.23258

Robb, J. (2016). What can we really say about skeletal part representation, MNI and funerary ritual? A simulation approach. *Journal of Archaeological Science: Reports*, *10*, 684–692. https://doi.org/10.1016/j.jasrep.2016.05.033

Saunders, S. R., & Barrans, L. (1999). What can be done about the infant category in skeletal samples? In R. D. Hoppa & C. M. Fitzgerald (Eds.), *Human growth in the past: Studies from bones and teeth* (pp. 183–209). Cambridge University Press.

Schattmann, A., Bertrand, B., Vatteoni, S., & Brickley, M. (2016). Approaches to co-occurrence: Scurvy and rickets in infants and young children of 16-18th century Douai, France. *International Journal of Paleopathology*, *12*, 63–75. https://doi.org/10.1016/j.ijpp.2015.12.002

Scheuer, L., & Black, S. (2000). *Developmental juvenile osteology*. Academic Press.

Schultz, M. (1987). The human skeletal remains from late PPNB Basta Southern Jordan. A preliminary report, in: H. J. Nissen, M Muheisen, H. G. Gebel: Report on the first two seasons of excavations at Basta (1986–1987). *Annual of the Department of Antiquities of Jordan*, *31*, 96–97. Retrieved from. http://publication.doa.gov.jo/Publications/ViewChapterPublic/1790

Schultz, M. (1993). *Vestiges of non-specific inflammation in prehistoric and historic skulls: A contribution to palaeopathology*. Anthropologische Beitrage.

Scrimshaw, N. S. (2003). A note from the outgoing editor. *Food and Nutrition Bulletin*, *24*(3), 246–246. https://doi.org/10.1177/156482650302400302

Shopfner, C. E. (1966). Periosteal bone growth in normal infants: A preliminary report. *American Journal of Roentgenology*, *97*(1), 154–163. https://doi.org/10.2214/ajr.97.1.154

Skelton, R., Maixner, W., & Isaacs, D. (1992). Sinusitis-induced subdural empyema. *Archives of Disease in Childhood*, *67*(12), 1478–1480. https://doi.org/10.1136/adc.67.12.1478

Sloan, B., Kulwin, D. R., & Kersten, R. C. (1999). Scurvy causing bilateral orbital hemorrhage. *Archives of Ophthalmology*, *117*(6), 842–843. https://doi.org/10.1001/archopht.117.6.842

Smith, M., & Brickley, M. (2009). *People of the Long Barrows*. Stroud: The History Press.

Snoddy, A. M. E., Buckley, H. R., Elliott, G. E., Standen, V. G., Arriaza, B. T., & Halcrow, S. E. (2018). Macroscopic features of scurvy in human skeletal remains: A literature synthesis and diagnostic guide. *American Journal of Physical Anthropology*, *167*(4), 876–895. https://doi.org/10.1002/ajpa.23699

Snoddy, A. M. E., Halcrow, S. E., Buckley, H. R., Standen, V. G., & Arriaza, B. T. (2017). Scurvy at the agricultural transition in the Atacama desert (ca 3600–3200 BP): nutritional stress at the maternal-foetal interface? *International Journal of Paleopathology*, *18*, 108–120. https://doi.org/10.1016/j.ijpp.2017.05.011

Stark, R. J. (2014). A proposed framework for the study of paleopathological cases of subadult scurvy. *International Journal of Paleopathology*, *5*, 18–26. https://doi.org/10.1016/j.ijpp.2014.01.005

Stoddart, S., Barber, G., Duhig, C., Mann, G., O'Connell, T., Lai, L., … Malone, C. (2009). The human and animal remains. In C. Malone, S. Stoddart, D. Trump, A. Bonanno, T. Gouder, & A. Pace (Eds.), *Mortuary customs in prehistoric Malta: Excavations at the Brochtorff Circle at Xagħra (1987–1994)* (pp. 315–340). McDonald Institute for Archaeological Research.

Stoddart, S., Malone, C., Mason, S., Trump, B., & Trump, D. (2009). Tarxien phase levels: spatial and stratigraphic analysis and reconstruction. In C. Malone, S. Stoddart, A. Bonanno, D. Trump, T. Gouder, & A. Pace (Eds.), *Mortuary customs in prehistoric Malta: Excavations at the Brochtorff Circle at Xagħra (1987–1994)* (pp. 109–218). McDonald Institute for Archaeological Research.

Stoddart, S., Power, R. K., Thompson, J. E., Mercieca-Spiteri, B., McLaughlin, R., Pace, A., & Malone, C. (in press). *Temple people: Bioarchaeology, resilience and culture in prehistoric Malta*. McDonald Institute for Archaeological Research.

Stuart-Macadam, P. (1985). Porotic hyperostosis: Representative of a childhood condition. *American Journal of Physical Anthropology*, *66*(4), 391–398. https://doi.org/10.1002/ajpa.1330660407

Stuart-Macadam, P. (1989). Nutritional deficiency diseases: a survey of scurvy, rickets, and iron deficiency anemia. In M. Y. Iscan & K. A. R. Kennedy (Eds.), *Reconstruction of Life from the Skeleton* (pp. 201–222). New York: Liss.

Stuart-Macadam, P. (1992). Porotic hyperostosis: A new perspective. *American Journal of Physical Anthropology*, *87*(1), 39–47. https://doi.org/10.1002/ajpa.1330870105

Swerdloff, B. A., Ozonoff, M. B., & Gyepes, M. T. (1970). Late recurrence of infantile cortical hyperostosis (Caffey's disease). *American Journal of Roentgenology*, *108*, 461–467. https://doi.org/10.2214/ajr.108.3.461

Thompson, J. E. (2020). Heads, shoulders, knees and toes: Exploring bodies, body parts and personhood in late Neolithic Malta through funerary taphonomy (University of Cambridge). *University of Cambridge.*. https://doi.org/10.17863/CAM.50091

Thompson, J. E., Parkinson, E. W., McLaughlin, T. R., Barratt, R., Power, R. K., Mercieca-Spiteri, B., … Malone, C. (2020). Placing and remembering the dead in late Neolithic Malta: bioarchaeological and spatial analysis of the Xagħra Circle hypogeum, Gozo. *World Archaeology*, *52*, 71–89. https://doi.org/10.1080/00438243.2019.1745680

Thompson, J. E., Power, R. K., Mercieca-Spiteri, B., McLaughlin, T. R., Robb, J., Stoddart, S., & Malone, C. (in press). Reconstructing deathways at the Xagħra Circle and Xemxija Tombs through funerary taphonomy. In S. Stoddart, R. K. Power, J. E. Thompson, B. Mercieca-Spiteri, R. McLaughlin, A. Pace, & C. Malone (Eds.), *Temple people: Bioarchaeology, resilience and culture in prehistoric Malta*. McDonald Institute for Archaeological Research.

Tontisirin, K., Nantel, G., & Bhattacharjee, L. (2002). Food-based strategies to meet the challenges of micronutrient malnutrition in the developing world. *Proceedings of the Nutrition Society*, *61*(2), 243–250. https://doi.org/10.1079/PNS2002155

Ubelaker, D. H. (1989). *Human skeletal remains: Excavation, analysis, interpretation*. Taraxacum.

Walker, P. L., Bathurst, R. R., Richman, R., Gjerdrum, T., & Andrushko, V. A. (2009). The causes of porotic hyperostosis and cribra orbitalia: A reappraisal of the iron-deficiency-anemia hypothesis. *American Journal*

of Physical Anthropology, *139*(2), 109–125. https://doi.org/10.1002/ajpa.21031

Wapler, U., Crubézy, E., & Schultz, M. (2004). Is cribra orbitalia synonymous with anemia? Analysis and interpretation of cranial pathology in Sudan. *American Journal of Physical Anthropology*, *123*(4), 333–339. https://doi.org/10.1002/ajpa.10321

Weston, D. A. (2008). Investigating the specificity of periosteal reactions in pathology museum specimens. *American Journal of Physical Anthropology*, *137*, 48–59. https://doi.org/10.1002/ajpa.20839

Weston, D. A. (2009). Brief communication: Paleohistopathological analysis of pathology museum specimens: Can periosteal reaction microstructure explain lesion etiology? *American Journal of Physical Anthropology*, *140*(1), 186–193. https://doi.org/10.1002/ajpa.21081

Weston, D. A. (2012). Nonspecific infection in paleopathology: Interpreting periosteal reactions. In A. L. Grauer (Ed.), *A companion to paleopathology* (pp. 492–512). Wiley-Blackwell.

How to cite this article: Thompson, J. E., Power, R. K., Mercieca-Spiteri, B., Magnussen, J. S., Pardey, M., Buck, L. T., Stock, J. T., McLaughlin, T. R., Stoddart, S., & Malone, C. (2021). Analysis of periosteal lesions from commingled human remains at the Xagħra Circle hypogeum reveals the first case of probable scurvy from Neolithic Malta. *International Journal of Osteoarchaeology*, 1–20. https://doi.org/10.1002/oa.3040